

Journal Pre-proof

A time domain finite element approach based on time series estimation

Alireza Firoozfar, Bahman Ansari

PII: S0997-7538(18)30577-1

DOI: <https://doi.org/10.1016/j.euromechsol.2019.103900>

Reference: EJMSOL 103900

To appear in: *European Journal of Mechanics / A Solids*

Received Date: 21 July 2018

Revised Date: 10 September 2019

Accepted Date: 4 November 2019

Please cite this article as: Firoozfar, A., Ansari, B., A time domain finite element approach based on time series estimation, *European Journal of Mechanics / A Solids* (2019), doi: <https://doi.org/10.1016/j.euromechsol.2019.103900>.

This is a PDF file of an article that has undergone enhancements after acceptance, such as the addition of a cover page and metadata, and formatting for readability, but it is not yet the definitive version of record. This version will undergo additional copyediting, typesetting and review before it is published in its final form, but we are providing this version to give early visibility of the article. Please note that, during the production process, errors may be discovered which could affect the content, and all legal disclaimers that apply to the journal pertain.

© 2019 Published by Elsevier Masson SAS.



A Time Domain Finite Element Approach Based on Time Series Estimation

Alireza Firoozfar, Bahman Ansari

Department of civil engineering, Faculty of Geotechnics, University of Zanjan, Zanjan, Iran

* Corresponding Author (firoozfar@znu.ac.ir)

*Phone Number: +98 (0) 24 3305 4207

Abstract

This paper details the use of time series for solving finite element equations. It was aimed at eliminating the discretization of time intervals to reduce calculation time and to obtain accurate results using time-dependent variables. For this purpose, the matrix form of the time series finite element formulation for both continuous and discontinuous time functions were extracted using Taylor and Fourier series for estimating time-dependent functions. Based on the extracted formulation, for solving elastodynamic problems, a computer code and algorithm was introduced. The efficiency and accuracy of the formulation was evaluated by solving different analytical examples. To reveal the power of time series for modeling real problems three practical examples such as settlement, flood protector structures and temporary cofferdams were modeled using time series approach and the results of analyses were presented. The results showed that having removed time discretization procedure, the time series based finite element method can be efficiently applied to decrease the calculation time and computational efforts. In addition, time-continuous responses resulting from this method, help reduce the calculation steps which is vital in many engineering problems.

Keywords: Finite Element Method, Time Series, Dynamic Analysis, Elasticity

1. Introduction

For more than fifty years, finite element analysis is a well-known approach for many researchers in different fields of science and industry [1-8]. Although the first developments of the discrete analysis go back to Newton [9] during the 16th century, the existence of finite element analysis was not considered before the development of the virtual work principle. The concepts of the virtual work principle return to the 17th and 18th centuries when Schellbach [10] made first analytical procedures, and Strutt [11] obtained numerical results for several problems. In elasticity, Ritz [12] showed a discrete approach for analyzing the Kirchhoff plate. The first use of triangular and rectangular elements for a two-dimensional Saint-Venant torsion problem was done by Courant [13]. The Modern shape of finite element method for analyzing structural and aeronautical problems was made by Turner et al. [14], Argyris [15] and Zienkiewicz [16, 17].

Over the last three decades, the development of computing devices has given a rapid growth to the use of finite element analysis for solving the engineering problems. In analyzing complex problems however, the slow solving process can be noted as a serious challenge. As an example, the dynamic analysis of the complex structures under earthquake loading usually takes hours to give accurate results [18]. To tackle this problem, several solutions have been proposed, among which the combination of finite element method with boundary element or discrete element methods can be cited [19-22]. Although combined

methods reduce the number of meshes, but in most applications, they lead to a complex formulations. The use of super computers [18, 23] and algorithm modifications [24] are another solutions for improving the results of finite element analysis. Super computers provide parallel computing in the same time which increases the calculation speed. However, they are expensive and in most applications they aren't economically feasible. Finite element results improvement using analytical modifications is another solution that can provide a cost effective and reliable approach for solving finite element problems. For instance Hayata et al. [25] used an extrapolation method for improving the accuracy of finite element analysis and reducing calculation time. Using Hamilton's law of varying action, Pitarresi and Manolis [26] introduced a method in which both spatial and temporal domains are interpolated via special shape functions leading to accurate results. Patnaik et al. [27] improved the accuracy of finite element dynamic analysis using integrated force method. Maan et al. [28] developed a fixed grid finite element method for the solution of eigenvalue problems using 4 and 20 nodes shell elements. Gupta et al. [29] extended a two-scaled generalized finite element method (GFEM) to solve three-dimensional fracture problems.

When the equilibrium equation involves velocity, acceleration and time-dependent boundary conditions, a time step procedure is required to discretize and solve the problem. In this way, using an appropriate number of spatial and time intervals, the solution gives an accurate result. This process is called multistep or stepwise procedure [30] which is a basis for finite element discretization. For a long-time needed analysis, however, discretizing of time intervals takes large time and more computational efforts. This is also the case for a problem with the complexly time-dependent boundary conditions.

An alternative method for traditional time step discretization is introduced using continuous time series. In this method, time-dependent vectors and all boundary and initial conditions are converted to continuous time series. In mathematics the use of series for solving ordinary differential equations is known as Frobenius method [31] which is also used for solving partial and nonlinear differential equations [32]. For the finite element analysis, time series eliminates the discretizing of time intervals and also, provides more accurate results using continuous time-dependent variables. This paper explains the way of using time series for shaping linear and non-linear finite element matrixes and presents a computer algorithm applied for solving several practical examples evaluating the efficiency of the used time series.

2. Finite Element Formulation

The elastodynamic equilibrium equation in finite element analysis is extracted using the virtual work principal as follows [30]:

$$KU_N(t) + C\dot{U}_N + M\ddot{U}_N(t) = P_N(t) \quad (1)$$

where U_N is the nodal displacement vector, \dot{U}_N and \ddot{U}_N are the nodal acceleration and velocity vectors respectively, K stands for the stiffness matrix, M shows the mass matrix, C represents damping matrix and P_N is the time-dependent force vector. The stiffness and mass matrix for equation (1) can be calculated by following equations [30]:

$$K = \int_V B^T D B dV \quad (2)$$

$$M = \int_V \rho \varphi^T \varphi dV \quad (3)$$

in which φ is the shape function matrix and B is the spatial derivatives of φ . D stands for a matrix associated with material properties and ρ is the density. According to Rayleigh damping theory [33], the damping matrix $[C]$ can be written as a combination of stiffness and mass matrixes as follows:

$$C = \alpha M + \beta K \quad (4)$$

where α and β are the Rayleigh constants which can be calculated by modal analysis of the problem [33].

3. Time Series Implementation

3.1. Continuous Time functions

Equation (1) gives a system of equations which contains all nodal variables. Considering the power of time series in time-dependent problem solution, especially their efficiency in reducing calculation time, a set of time series is considered for solving equation (1) as an alternative way to traditional methods. For a time domain finite element analysis, all nodal variables can be estimated with continuous time functions using a set of time series. Therefore, for a given node i the displacement and force vector can be estimated by time series as follows:

$$U^i(t) = \sum_{j=0}^{NES} a_j^i (t - t_0)^j \quad (5)$$

$$P^i(t) = \sum_{j=0}^{NES} p_j^i (t - t_0)^j \quad (6)$$

In which a_j^i and p_j^i are the j 's coefficients of the series for node i and NES is the number of used coefficients. Equations (5) and (6) represent the Taylor series for the given functions $U(t)$ and $P(t)$ around the time t_0 [34]. For obtaining velocity and acceleration vectors, the first and the second derivatives from equation (5) are taken as follows:

$$\dot{U}^i(t) = \sum_{j=1}^{NES} j a_j^i (t - t_0)^{j-1} \quad (7)$$

$$\ddot{U}^i(t) = \sum_{j=2}^{NES} j(j-1) p_j^i (t - t_0)^{j-2} \quad (8)$$

By substituting equations (5), (6), (7) and (8) in equation (1) the following equation can be extracted:

$$\begin{aligned}
K \sum_{j=0}^{NES} a_j^i (t - t_0)^j + C \sum_{j=1}^{NES} j a_j^i (t - t_0)^{j-1} + M \sum_{j=2}^{NES} j(j-1) p_j^i (t - t_0)^{j-2} \\
= \sum_{j=0}^{NES} p_j^i (t - t_0)^j
\end{aligned} \tag{9}$$

in which by separating $(t - t_0)^j$ coefficients in both sides of the equation, the matrix form can be written as follows:

$$[K_{N \times N}] [a_j^i]_{N \times 1} + [C_{N \times N}] [(j+1)a_{j+1}^i]_{N \times 1} + [M_{N \times N}] [(j+2)(j+1)a_{j+2}^i]_{N \times 1} = [p_j^i]_{N \times 1} \tag{10}$$

where a_j^i are the unknown coefficients of the time series and N is equal to $3NN$ and $2NN$ for 3dimensional and 2dimensional cases respectively (NN is the number of nodes). The equation (10) can be arranged in a matrix as follows:

$$\begin{bmatrix}
[K] & [C] & [2M] & 0 & 0 & 0 & 0 \\
0 & [K] & [2C] & [6M] & 0 & 0 & 0 \\
0 & 0 & [K] & [3C] & [12M] & 0 & 0 \\
\vdots & \vdots & \vdots & \vdots & \vdots & \vdots & \vdots \\
0 & 0 & 0 & 0 & 0 & [K] & [(NES-1)C] \\
0 & 0 & 0 & 0 & 0 & \dots & [K]
\end{bmatrix}
\begin{bmatrix}
[a_0] \\
[a_1] \\
[a_2] \\
\vdots \\
[a_{NES}]
\end{bmatrix}
=
\begin{bmatrix}
[p_0] \\
[p_1] \\
[p_2] \\
\vdots \\
[p_{NES}]
\end{bmatrix} \tag{11}$$

In which $[a_j]$ are the unknown series coefficients. Equation (11) can be used for solving a finite element problem, when the number of elements is small. In contrast, a complex and large geometry model requires a large number of elements therefore, the needed computational space for storing equation (11) hugely increases. To overcome this problem, the unknown series coefficients can be obtained separately by starting the solution process from the last row of the equation (11) as follows:

$$\{a_{NES}\} = [K]^{-1} \{p_{NES}\} \tag{12}$$

After obtaining a_{NES} coefficients, the a_{NES-1} coefficients can be achieved separately as follows:

$$\{a_{NES-1}\} = [K]^{-1} \{p_{NES-1}\} - [(NES-1)C] \{a_{NES}\} \tag{13}$$

And this process is continued for obtaining all unknown series coefficients in the NES number of steps.

3.2. Discontinuous Time Functions

Taylor series function shown in equation (5) can often be appropriately applied to solve the equation (1), however, for some problems, the solution may face some difficulties. For instance, when the boundary and initial conditions are associated with high-frequency functions such as earthquakes, or they are defined by discontinuous or broken functions, the number of coefficients in Taylor series should be increased to obtain an accurate result which may lead to more time consumption. For such problems, another form of time series called Fourier series [35] can be used. The Fourier series is a common series

for analyzing problems associated with discontinuous functions. A periodic time-dependent function $U(t)$ can be estimated by a Fourier series as follows:

$$U(t) = \frac{1}{2}a_0 + \sum_{j=1}^{NES} a_j \cos\left(\frac{j\pi t}{l}\right) + b_j \sin\left(\frac{j\pi t}{l}\right) \quad (14)$$

$$P(t) = \frac{1}{2}p_0^c + \sum_{j=1}^{NES} p_j^c \cos\left(\frac{j\pi t}{l}\right) + p_j^s \sin\left(\frac{j\pi t}{l}\right) \quad (15)$$

In which, l is the half period of the functions and a_j (or p_j^c), and b_j (or p_j^s) are the series coefficients which can be calculated using following equations:

$$a_j \text{ or } p_j^c = \frac{1}{l} \int_{-l}^l [U(t) \text{ or } P(t)] \cos\left(\frac{j\pi t}{l}\right) dt \quad (16)$$

$$b_j \text{ or } p_j^s = \frac{1}{l} \int_{-l}^l [U(t) \text{ or } P(t)] \sin\left(\frac{j\pi t}{l}\right) dt \quad (17)$$

After differentiating equation (13) and substituting the results in equation (1), the following equations can be obtained:

$$[K_{N \times N}] [a_j^c]_{N \times 1} = [p_j^c]_{N \times 1} \quad \text{for } j = 0 \quad (18)$$

$$\begin{bmatrix} K - \frac{j^2 \pi^2}{l^2} M & j \frac{\pi}{l} C \\ -j \frac{\pi}{l} C & K - \frac{j^2 \pi^2}{l^2} M \end{bmatrix}_{2N \times 2N} \begin{bmatrix} a_j^i \\ b_j^i \end{bmatrix}_{2N \times 1} = \begin{bmatrix} p_j^{ci} \\ p_j^{si} \end{bmatrix}_{2N \times 1} \quad \text{for } j > 0 \quad (19)$$

where a_j and b_j are the coefficients of $\cos(j\pi t/l)$ and $\sin(j\pi t/l)$ for nodal displacements, respectively, and p_j^c and p_j^s are the same coefficients for nodal forces. The matrix form of the equations (18) and (19) can be written as follows:

$$\begin{bmatrix} [K] & 0 & 0 & 0 & 0 \\ 0 & \left[K - \frac{\pi^2}{l^2} M \right] & \left[\frac{\pi}{l} C \right] & 0 & 0 \\ 0 & \left[-\frac{\pi}{l} C \right] & \left[K - \frac{\pi^2}{l^2} M \right] & 0 & 0 \\ \vdots & \vdots & \vdots & \vdots & \vdots \\ 0 & 0 & 0 & \left[K - NES^2 \frac{\pi^2}{l^2} M \right] & \left[NES \frac{\pi}{l} C \right] \\ 0 & 0 & 0 & \left[-NES \frac{\pi}{l} C \right] & \left[K - NES^2 \frac{\pi^2}{l^2} M \right] \end{bmatrix} \begin{bmatrix} [a_0] \\ [a_1] \\ [b_1] \\ \vdots \\ [a_{NES}] \\ [b_{NES}] \end{bmatrix} = \begin{bmatrix} [p_0] \\ [p_1^c] \\ [p_1^s] \\ \vdots \\ [p_{NES}^c] \\ [p_{NES}^s] \end{bmatrix} \quad (20)$$

Previously used direct harmonic analysis [36] which gives the displacements as a summation of harmonic functions can be categorized under the Fourier series finite element analysis.

3.3. Non-Linear Time series Finite element analysis

When the relation between stress and strain is non-linear, it can be shown that the equation (1) can be rewritten as follows:

$$M\Delta\ddot{U}^{i+1} + C\Delta\dot{U}^{i+1} + K^*\Delta U^{i+1} + M\ddot{U}^i + C\dot{U}^i + F^i = P(t) \quad (21)$$

in which K^* is the non-linear stiffness matrix and F^i is the internal force vector at iteration i . The non-linear stiffness matrix and the force vector can be calculated as follows [30]:

$$K^* = \int_V B^T D^* B dV \quad (22)$$

$$D^* = \frac{\partial \sigma(\varepsilon)}{\partial \varepsilon} \Big|_{\varepsilon^i} \quad (23)$$

$$F^i = \int_V B^T \sigma(\varepsilon^i) dV \quad (24)$$

where ε^i is the strain at iteration i and $\sigma(\varepsilon)$ is the stress as a function of strain. If the nodal displacement and force vectors are estimated by a Taylor series, the equation (21) can be written as:

$$\begin{aligned} K^{*i}(t_j)\Delta a_0^{i+1} + (K^{*i}(t_j)(t_j - t_0) + C)\Delta a_1^{i+1} + \dots \\ + (K^{*i}(t_j)(t_j - t_0)^{NES} + NES(t_j - t_0)^{NES-1}C \dots \\ + NES(NES - 1)(t_j - t_0)^{NES-2}M)\Delta a_{NES}^{i+1} = G^i(t_j) \end{aligned} \quad (25)$$

in which $K^{*i}(t_j)$ is the non-linear stiffness matrix at time t_j in iteration i , C is the damping matrix, M is the mass matrix and $\Delta a_k^{i+1} = a_k^{i+1} - a_k^i$ is the series coefficients difference vector. $G^i(t_j)$ are the time-dependent values which can be calculated as follows:

$$G^i(t_j) = P(t_j) - F^i(t_j) - M\ddot{U}^i(t_j) - C\dot{U}^i(t_j) \quad (26)$$

Using the concept of Least Square Method [37], for all t_j that are perfectly chosen around t_0 , there are sets of equations similar to equation (25) which when $NF(\geq NES + 1)$ number of t_j are chosen, the best values for Δa_k^{i+1} can be calculated by minimizing below error function:

$$E = \left\| A^i \{ \Delta a \}^i - G^i \right\|^2 \quad (27)$$

where A is the coefficient matrix that can be extracted from equation (25) as follows:

$$A = \begin{bmatrix} K^{*i}(t_1) & K^{*i}(t_1)dt_1 + C & \dots & K^{*i}(t_1)dt_1^{NES} + NESdt_1^{NES-1}C + NES(NES - 1)dt_1^{NES-2}M \\ \vdots & \vdots & \vdots & \vdots \\ K^{*i}(t_{NF}) & K^{*i}(t_{NF})dt_{NF} + C & \dots & K^{*i}(t_{NF})dt_{NF}^{NES} + NESdt_{NF}^{NES-1}C + NES(NES - 1)dt_{NF}^{NES-2}M \end{bmatrix} \quad (28)$$

in which $dt_j = t_j - t_0$ is the time difference values. By using a Least Square Solution [37] for minimizing the error function (27), the values for the coefficient differences at iteration $i + 1$ can be calculated as follows:

$$\{\Delta a^{i+1}\} = (A^{iT} A^i)^{-1} A^{iT} G^i \quad (29)$$

And finally, the series coefficients for iteration $i + 1$ can be calculated:

$$\{a^{i+1}\} = a^i + \Delta a^{i+1} \quad (30)$$

where a^i are the series coefficients for iteration i .

Below algorithm shows the way of implementing non-linear time series for a finite element analysis:

- 1- Choose initial coefficients at iteration i (a^i) (It is necessary to use the initial conditions for forming a^i when better convergence is required. For example if the initial displacement for a node j at time t_0 is zero, the a_0 coefficient for this node must be equal to zero for all iterations and t_j s).
- 2- Choose a number of $t_j \geq 0$ around t_0 ($j = 1$ to $NF \geq NES + 1$)
- 3- Calculate $U^i, \dot{U}^i, \ddot{U}^i$ by using equations (5), (7) and (8) respectively.
- 4- Calculate ε^i by using following equation (B is the spatial derivatives of shape functions [30]):

$$\varepsilon^i = B U^i \quad (31)$$

- 5- Calculate $K^{*i}(t_j)$ and $F^i(t_j)$ for each t_j at iteration i using equations (22) and (24), respectively.
- 6- Calculate $G^i(t_j)$ and A^i for each t_j using equations (26) and (28), respectively.
- 7- Calculate Δa^{i+1} using equation (29).
- 8- Calculate series coefficients at iteration $i + 1$ (a^{i+1}) using equation (30).
- 9- Check if the Δa^{i+1} is lesser than a threshold(δ).
- 10- If the answer of step (6) is Yes, end the calculation else, return to step 3 and continue calculation until the Δa^{i+1} become lesser than δ .

For complex problems with large number of elements, it is possible to discrete the A matrix to calculate the first four series coefficients a_0, a_1, a_2 and a_3 and then use the obtained results to calculate other coefficients.

Equations (11), (19) and (29) emerged from time series based finite element dynamic analysis, owns some significant advantages compared to that of traditional methods. First, solving of these equations is

not dependent on the time step discretization. In fact, the time domain analysis in traditional finite element method is based on time interval discretization of time-dependent components such as velocity and acceleration vectors. In this process, time steps are interdependent such that using a time step procedure, the unknowns of each step can be calculated by applying the results from the previous step to current step. This dependency leads to a time-consuming solution for analysis containing long time intervals to obtain proper results. In contrast, time series finite element analysis can efficiently reduce the solution time because, in this method, input and output variables are continuous time functions giving desired values with lesser computational efforts.

As the second advantage, the accuracy of this method can be marked. With the application of time series, the nodal displacements are obtained as continuous time functions and can analytically be integrated and differentiated giving more accurate results than numerical methods.

3.4. TSFEM Algorithm

To evaluate the introduced time series finite element formulation a computer code called TSFEM (Time Series Finite Element Method) was written in Matlab environment. This code uses eight nodes element for time domain analysis of 2dimensional plane strain and plane stress problems. The schematic flow diagram of the developed algorithm is shown in figure (1). According to this figure, necessary input variables of the algorithm are nodal coordinates, code vector which defines the type of boundary conditions for each node (Prescribed Displacement=0, Prescribed Force=1), time series coefficients for prescribed boundary values, material properties (Elastic modulus (E), Poisson ratio (ν), density (ρ), Rayleigh damping coefficients (α, β)).

Figure (1) depicts that, after reading the input variables at the first step, the K , C and M matrixes are formed based on the finite element formulation. These matrixes are then added up to the left side matrixes (A) of equations (11) and (19) based on Taylor or Fourier series formulations, respectively. After rearranging all known (F) and unknown (X) vectors, the unknown vector can be computed by multiplying the inverse of A matrix to F vector. When the time series coefficients were computed for each node, the displacement can be calculated by using equation (5) or (13).

4. Validation examples

4.1. Beam under harmonic base motion

The use of TSFEM for computing natural frequencies of a cantilever beam is considered as the first evaluation example. Figure (2a) shows the boundary conditions of the problem. The beam length and height are 20m and 4m, respectively and its width is 1m. It is made of steel with $E = 2.08e + 5 \text{ Mpa}$, $\nu = 0.3$, $\rho = 7800 \text{ kg/m}^3$ and $\alpha = \beta = 0$. The harmonic motion is applied on the base of the beam as sinusoidal unit amplitude motions with different ω angular frequencies. This harmonic motion can be converted to a Fourier series with $a_j = 0$, $b_1 = 1$, $b_{j \neq 1} = 0$ and $l = \pi/\omega$. The number of twenty, 8 nodes element and 2 Fourier and 10 Taylor series coefficients were used for solving the problem. Figures (2b) shows the amplitudes of the middle point of the beam's extreme (point A) with respect to different

values of angular frequencies. As can be seen in this figure the accuracy of the TSFEM algorithm is in a good agreement with an analytical solution [38].

4.2. Plate under Uniform Traction

Previous example showed the efficiency of TSFEM algorithm for analyzing the harmonic motions. As the second instance, a square plate under uniform traction on its side was analyzed by TSFEM (Figure 3a). The plate length and thickness are 6m and 1m, respectively. The material properties of the plate are as $E = 2.5Mpa$, $\nu = 0.25$, $\rho = 100 kg/m^3$ and $\alpha = \beta = 0$. According to the figure (3a), for modeling harmonic traction sinusoidal traction with amplitude $100 N/m^2$ and different ω angular frequencies were applied on one side of the plate along y -direction. The number of sixteen 8 nodes element with 2 Fourier and 10 Taylor series coefficients was used for calculating frequency response of the plate. Figure (3b) shows a comparison between the analytical and numerical displacements at the point A . As can be seen, there is a good agreement between analytical [38] and numerical solutions.

5. Practical Examples

5.1. Soil settlement due to reservoir impoundment

The TSFEM application is more effective when the time-continuous responses are needed. For example, when a water reservoir (figure 4) is impounded, the soil beneath settles due to vertical loading. Modeling such problems with stepwise finite element procedures take long time because, impounding is a slow process and therefore, the number of required time steps notably increase. It is possible to model the pressure function with both Taylor and Fourier series. In a continuous Taylor model for node i , the pressure increment can be shown as a linear function:

$$p^i(t) = \frac{\gamma_w Q}{A} t \quad (32)$$

where Q (m^3/s) is volumetric flow rate, γ_w (N/m^2) is the water unit weight, A (m^2) is the reservoir area and t stands for the time. For equation (20), the Taylor series coefficients can be set as $a_{j \neq 1} = 0$ and $a_1 = \frac{\gamma_w Q}{A}$. Although this equation shows a pressure increment on the bottom of the reservoir, it doesn't consider the nature of the loading. In fact, the pressure caused by impounding will increase until a specific time t_{max} , and after that it becomes constant. This type of time function can be expressed with a broken function as follow:

$$p^i(t) = \begin{cases} \frac{\gamma_w Q}{A} t & 0 \leq t < t_{max} \\ \gamma_w h_{max} & t_{max} < t \end{cases} \quad (33)$$

In this case, for accurately modeling of pressure change, a Fourier series with 30 coefficients can be used.

Figures (5a) and (5b) illustrate the results of Taylor series model for the settlement of a sandy soil when the pressure increases with time. A linear relation can be seen between settlement and time, and the maximum settlement occurs when the time reaches $t = t_{max}$. Maximum settlement occurs beneath the midpoint of the reservoir, and at this point, the settlement rate is faster than others. Obviously, the rate of settlement increases with the increasing volumetric flow rate (Q) shown in figure (5b). Figures (5c) and (5d) show the Fourier model of the settlement. Although the Taylor series appropriately models the settlement until $t = t_{max}$, the behavior of settlement cannot be seen after t_{max} . Whereas, this behavior can be expressed by a Fourier series. According to figures (5c) and (5d), Fourier model shows the same results as Taylor series showed. However, in addition, this model can show the behavior of settlement after the period of impoundment.

For comparing time series computational efforts with a stepwise finite element solution, the settlement problem was also solved by a stepwise finite element procedure and the number of 1500 time steps with 0.01sec time intervals were used to reach the proper results. In contrast, time series by Taylor model only took 2 computational steps, and Fourier series took 30 computational steps for solving this problem.

5.2. Flood protection sheet pile

Steel sheet piles have been utilized for more than 100 years, as reliable and cost-effective solution for problems like the construction of temporary cofferdams. Steel sheet piles have also been widely used in riverine flow control structures and flood defense systems. They have traditionally been used for the protection of river banks, and flood protection. Ease of use, the speed of execution, long service life and the ability to be driven in the water make sheet piles a proper choice for permanent and temporary structures. The loading regime behind the structure cost-effectively impacts the design of sheet piles. Through traditional methods, the load of flood or other effective loads is statically computed, but in fact, loading is time-dependent and this must be taken into account in designing. Furthermore, traditional ways of numerical modeling may have trouble with the slow rate of the loading. In contrary, for modeling of such problems, the use of time series can give effective solutions.

When the construction of a flood protection sheet pile is completed, the pressure behind it increases during the flood (Figure 5). Considering figure (5), for a node i on the sheet pile wall, the pressure varies with time as follows:

$$p^i(t) = \begin{cases} 0 & 0 < t \leq t_i \\ \gamma_w \left(\frac{Q}{A} t - y_i \right) & t_i < t \leq t_{max} \\ \gamma_w (h_{max} - y_i) & t_{max} < t \end{cases} \quad (34)$$

where t_i is the time at which the water reaches node i and y_i is the height of the node. The water reaches its maximum allowable height (h_{max}) at the time $= t_{max}$. Equation (22) can be accurately estimated by a Fourier series with 30 coefficients. Figure (7) shows the behavior of the sheet pile during the flood. This figure gives the speed and displacement of each node of the wall at any time. For modeling this problem with stepwise finite element analysis, the number of 2000 time steps with 10sec time intervals were required. However, time series finite element solved this problem only with 30

series coefficients and much lesser computational efforts. According to Figure (7), the displacement response of the sheet pile is a nonlinear function with an increasing trend until the water reaches its maximum allowable height (h_{max}). The speed of reaching to the maximum displacement for each node of the wall side depends on the both volumetric flow rate (Q) and height of the node (y_i) from the base. According to figures (7a) and (7b) by doubling the volumetric flow rate, the time of reaching the maximum displacement halves. When the wall thickness is 5cm the maximum displacement heads to 5.5cm and a thickened wall shows a reduction in displacement declining to a value of 7mm. For all cases, the deformation is about zero, an hour after the beginning of the flood. The time of zero deformation is dependent on the volumetric flow rate (Q), maximum allowed height (h_{max}) and the thickness of the wall (d).

5.3. Cofferdam Sheet pile wall

A cofferdam is a structure temporally built to keep water or soil out for dewatering. Therefore a dry environment is provided for construction. Figure (8) shows the two sides of a sheet pile cofferdam. When the construction of the cofferdam is completed, the water starts to be pumped out, from the side A. This process increases the pressure on the wall nodes at side B. According to figure (8), for a node i , the pressure increment can be written as follows:

$$p^i(t) = \begin{cases} \gamma_w \left(\frac{h_{max}}{t_i} - \frac{Q}{A} \right) t & 0 < t \leq t_i \\ \gamma_w (h_{max} - y_i) & t_i < t \end{cases} \quad (35)$$

in which h_{max} is the maximum water height in side A and t_i is the time when the water level reaches to the node i . Q is the volumetric flow rate and A represents the inside area of the cofferdam. For modeling this problem a Fourier series with 30 series coefficients were used. The same model was solved by a stepwise finite element procedure with the number of 2000 time steps and 10sec time intervals. Figure (9) shows the time series results of horizontal deformation of the wall with respect to time. The behavior of cofferdam deformation differs from flood protecting sheet piles. In this case, the displacement increases with time and the speed of reaching the maximum displacement in high elevated nodes is more than low elevated nodes. But, with the time passing this speed decreases and finally, after the time $t = t_{max}$ the displacements cease and reach constant amounts exactly indicating the behavior of the wall deformation over the time.

6. Conclusion

In this paper, a method based on time series formulation was presented as a new scheme for solving finite element equations. The main concept of using time series for discretizing time intervals rises from the fact that the traditional stepwise procedures in finite element method cause some difficulties for solving modern problems related to complex structures as much seen in civil and mechanical engineering. In traditional methods most physical phenomena are modeled stepwise and the behavior of models are related to previous steps. This means, if the behavior of model is needed after a long time, it is required to know all past behaviors of model which is time consuming in most modern problems.

However, using time series concept, a new window for solving these kind problems can be opened. With using of continuous time series, it is not required to discrete time intervals. This allows us to calculate the behavior of model in any time without considering previous steps. In this paper three time-consuming geotechnical problems such as settlement, flood protector wall and cofferdam were modeled by time series formulation. In all models the time series gave the accurate results only using a few number of time steps. For example in modeling settlement due to impoundment of a reservoir with traditional stepwise procedures averagely 1500 time steps with 0.01sec time intervals were used, while the same problem was solved by using time series with 2 series coefficients only in 2 steps. Or when modeling flood protector wall, the deformation of the wall during the flood was calculated using 2000 time steps in traditional procedures whereas time series solved the same problem only in 30 time steps. The same results obtained when the pressure of the pumping out the water behind a cofferdam was modeled by time series finite element formulation.

Another important advantage of time series formulation is the time- continuous responses that can be directly extracted from the results of the calculation. This concept allows us to provide mathematical procedures as rapid as possible and because of continuity of the results the differentiation and integration will be more accurate. By solving two validation examples, for evaluating the accuracy of time series formulation the problem of wave propagation inside a solid body was modeled. The results obviously showed the power of time series formulation for solving finite element problems and demonstrated that the use of this procedure can significantly decrease calculation time and provide more accurate results.

7. References

- [1] Yu SH, Houlsby GT. A new finite element formulation for one-dimensional analysis of elastic-plastic materials. *Computers and Geotechnics*. 1990; 241:256-9.
- [2] Abdelatif AO, Owen JS, Hussein MFM. Modelling the prestress transfer in pre-tensioned concrete elements. *Finite Elements in Analysis and Design*. 2015; 47:63-94.
- [3] Zona A, Ranzi G. Finite element models for nonlinear analysis of steel–concrete composite beams with partial interaction in combined bending and shear. *Finite Elements in Analysis and Design*. 2011; 98:118-47.
- [4] Nguyen-Xuan H. A polygonal finite element method for plate analysis. *Computers & Structures*. 2017; 45:62-188.
- [5] Shang HY, Machado RD, Abdalla Filho JE. Dynamic analysis of Euler–Bernoulli beam problems using the Generalized Finite Element Method. *Computers & Structures*. 2016; 109:122-173;
- [6] Ching J, Phoon KK. Effect of element sizes in random field finite element simulations of soil shear strength. *Computers & Structures*. 2013; 120:134-126.
- [7] Moita JS, Araújo AL, Martins P, Mota Soares CM, Mota Soares CA. A finite element model for the analysis of viscoelastic sandwich structures. *Computers & Structures*. 2011; 1874:1881-89.

- [8] Tschuchnigg F, Schweiger HF, Sloan SW. Slope stability analysis by means of finite element limit analysis and finite element strength reduction techniques. Part II: Back analyses of a case history. *Computers and Geotechnics*. 2015; 178:189-70.
- [9] Stein E. History of the Finite Element Method – Mathematics Meets Mechanics – Part I: Engineering Developments. *The History of Theoretical, Material and Computational Mechanics*. 2014; 399:442.
- [10] Schellbach KH. Probleme der Variationsrechnung. *Crelle's Journal für die reine und angewandte Mathematik*. 1851; 293:363-41.
- [11] Strutt JW. *The theory of sound*, London; 1877.
- [12] Ritz W. Über eine neue Methode zur Lösung gewisser Probleme der mathematischen Physik. *Journal für die reine und angewandte Mathematik*. 1909; 1:61-135.
- [13] Courant R. Variational methods for the solution of problems of equilibrium and vibrations. *Bulletin of the American Mathematical Society*. 1943; 1:23-49.
- [14] Turner MJ, Clough RW, Martin HC, Topp LJ. Stiffness and deflection analysis of complex structures. *Journal of the Aeronautical Sciences*. 1956; 805:823-23.
- [15] Argyris JH. Energy theorems and structural analysis. *Aircraft Engineering*. 1955; 154:158.
- [16] Zienkiewicz O, Cheung Y. *The finite element method*. McGraw-Hill; 1967.
- [17] Zienkiewicz O, Taylor R. *The finite element method*. 5th ed. Butterworth-Heinemann; 2000.
- [18] Miyamura T, Akiba H, Hori M. Large-scale seismic response analysis of super-high-rise steel building considering soil-structure interaction. *International journal of High-rise buildings*. 2015; 4:75-83.
- [19] Meguro K, Tagel-Din H. *Applied element method for structural analysis: Theory and application for linear materials*. Japan Society of Civil Engineers. Japan; 2000.
- [20] Shirkol AI, Nasar T. Coupled boundary element method and finite element method for hydroelastic analysis of floating plate. *Journal of Ocean Engineering and Science*. 2018; 19:37-3.
- [21] Onate E, Rojek J. Combination of discrete element and finite element methods for dynamic analysis of geomechanics problems. *Computer Methods in Applied Mechanics and Engineering*. 2004; 3087:3128-193.
- [22] Rudolphi TJ, Lohmar W. A Combined Boundary and Finite Element Implementation for Axisymmetric Thermoelasticity. *Advanced Boundary Element Methods*. 1988; 379:387.
- [23] Merta M, Zapletal J, Brzobohaty T, Markopoulos A, Riha L, Cermak M, Hapla V, Horak D, Pospisil L, Vasatova A. Numerical libraries solving large-scale problems developed at IT4Innovations research programme supercomputing for industry. *Perspective in science*. 2016; 7:140-150.
- [24] Stark S, Roth S, Neumeister P, Balke H. Modifications of the Newton–Raphson method for finite element simulations in ferroelectroelasticity. *International Journal of Solids and Structures*. 2013; 50:773-780.

- [25] Hayata K, Koshiba M, Suzuki M. A method for improving the accuracy of finite-element solutions using the extrapolation method. *Electronics and Communications in Japan*. 1986; 38:47-69.
- [26] Pitarresi JM, Manolis GD. The temporal finite element method in structural dynamics. *Computers & Structures*. 1991; 647:655-41.
- [27] Patnaik SN, Hopkins DA, Aiello RA, Berke L. Improved accuracy for finite element structural analysis via an integrated force method. *Computers & Structures*. 1992; 521:542-45.
- [28] Maan FS, Querin OM, Barton DC. Extension of the fixed grid finite element method to eigenvalue problems. *Advances in Engineering Software*. 2007; 607:617-38.
- [29] Gupta V, Kim DJ, Duarte AC. Extensions of the two-scale generalized finite element method to nonlinear fracture problems. *International Journal for Multiscale Computational Engineering*. 2013; 581:596-11.
- [30] Bathe KJ. *Finite Element Procedures*. PRENTICE HALL. New Jersey; 1996.
- [31] Arfken G. *Mathematical Methods for Physicists*. 3rd edition. Orlando FL: Academic Press, 1985.
- [32] Nuseir A, Al-Hasoon A. Power series solution for nonlinear systems of partial differential equations. *Applied Mathematical science*. 2012; 6:5147-5159.
- [33] Mohammad DRA, Khan NU, Ramamurti V. On the role of Rayleigh damping. *Journal of Sound and Vibration*. 1995; 207:218-185.
- [34] Abramowitz M, Stegun I A. *Handbook of Mathematical Functions with Formulas, Graphs, and Mathematical Tables*. New York: Dover; 1972.
- [35] Askey R, Haimo DT. Similarities between Fourier and Power Series. *American Mathematical Monthly*. 1996; 297:304-103.
- [36] Genta G, Tonoli A. A harmonic finite element for the analysis of flexural, torsional and axial rotor dynamic behavior of blade arrays. *Journal of Sound and Vibration*. 1997; 207:693-720.
- [37] Rao C.R, Touternburg H, Heumann C. *Linear Models and Generalizations*. 3rd edition. Springer-Verlag Berlin Heidelberg, 2008.
- [38] Achenbach JD. *Wave Propagation in Elastic Solids*. North-Holland. Amsterdam; 1973.

Figures:

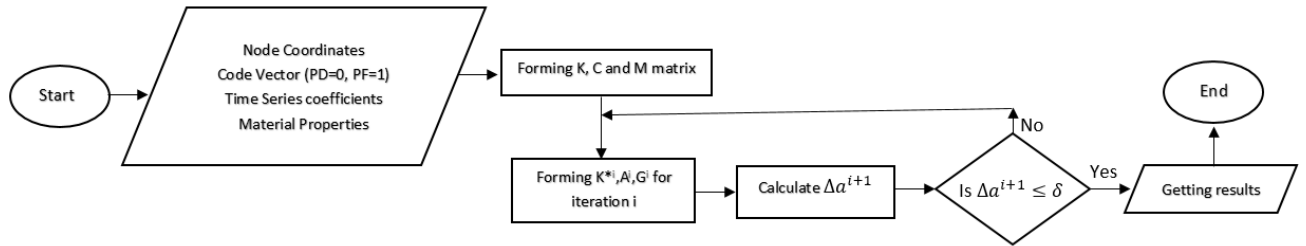


Figure 1- Flow diagram of TSFEM (Time Series Finite Element Method) algorithm

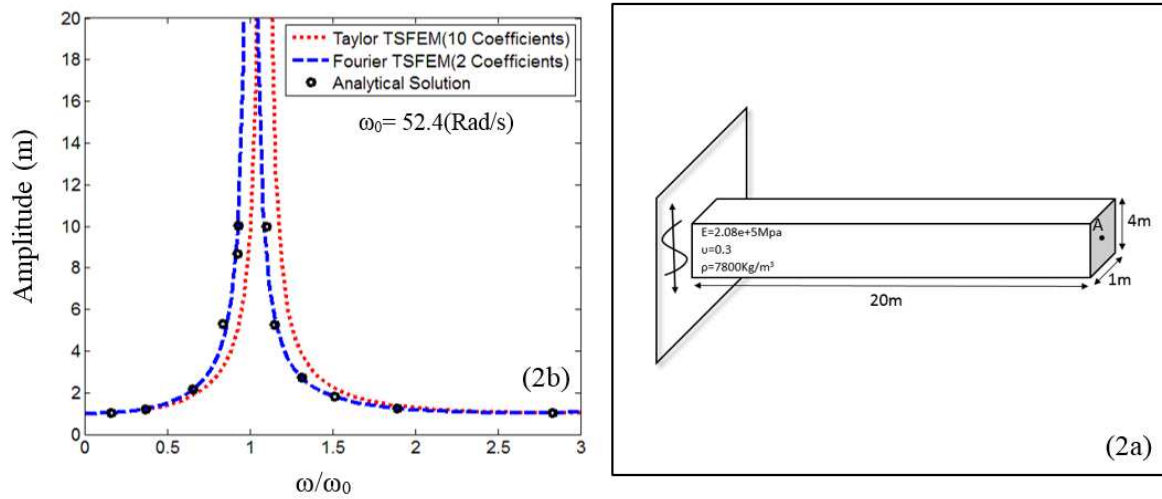


Figure 2- beam response to the harmonic base excitation. 2a) Schematic statement of the problem 2b) Amplitudes of beam's extreme point (Point A) with respect to different values of angular frequencies (ω_0 is the first natural frequency of the beam).

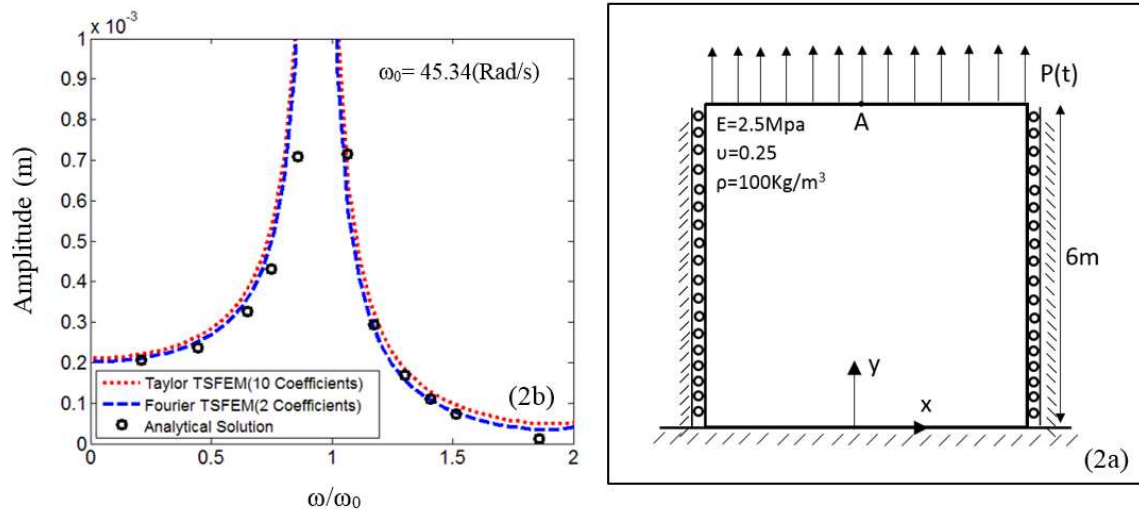


Figure 3- Plate response to the harmonic traction excitation on its side. 2a) Schematic statement of the problem 2b) Displacement amplitudes of plate's extreme point (Point A) with respect to different values of angular frequencies (ω_0 is the first natural frequency of the plate)

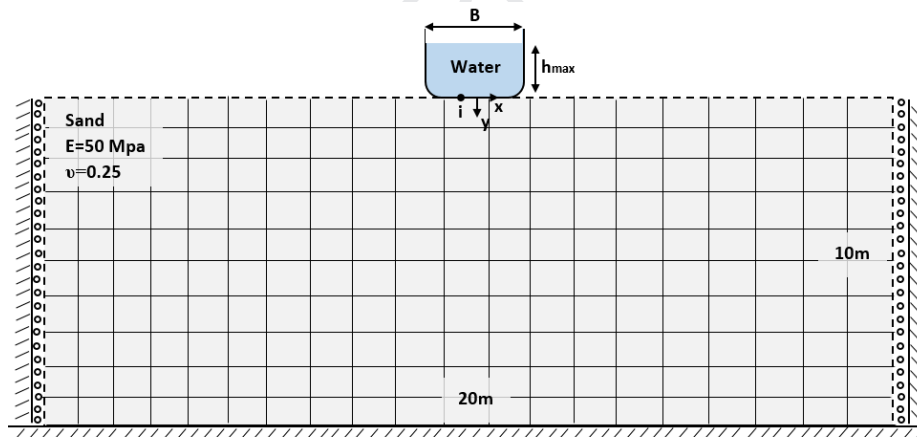


Figure 4- Model of a water reservoir constructed on a sandy soil

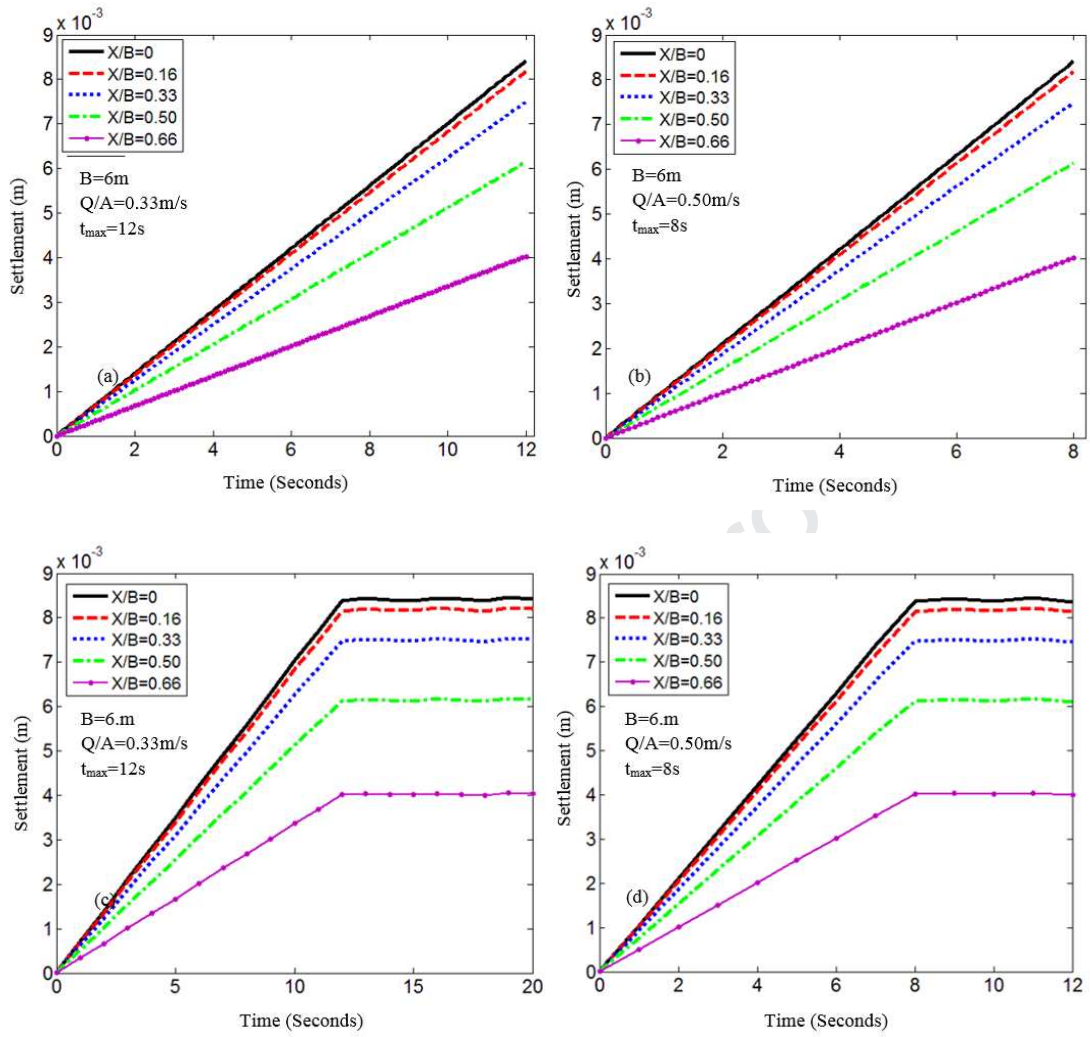


Figure 5- Settlement of a sandy soil beneath a reservoir due to impounding induced pressure with time.

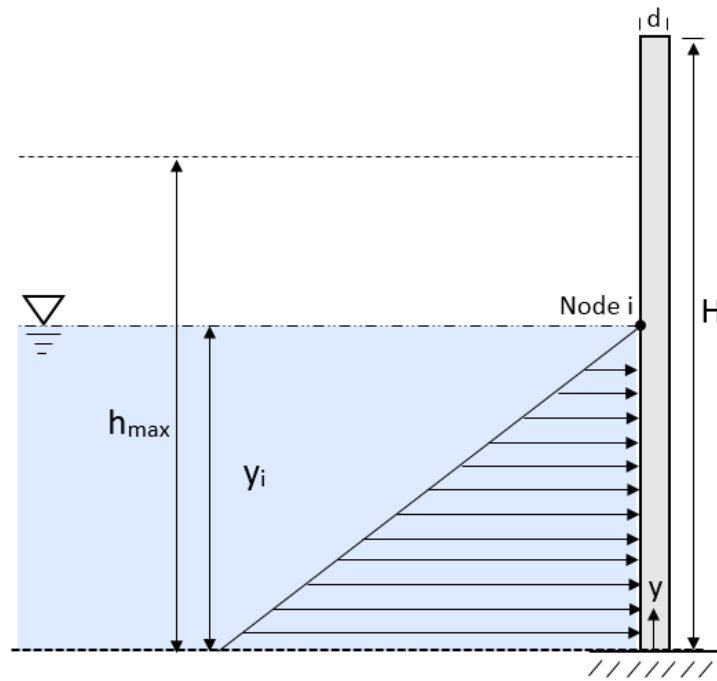


Figure 6- A flood protection sheet pile model for the TSFEM algorithm.

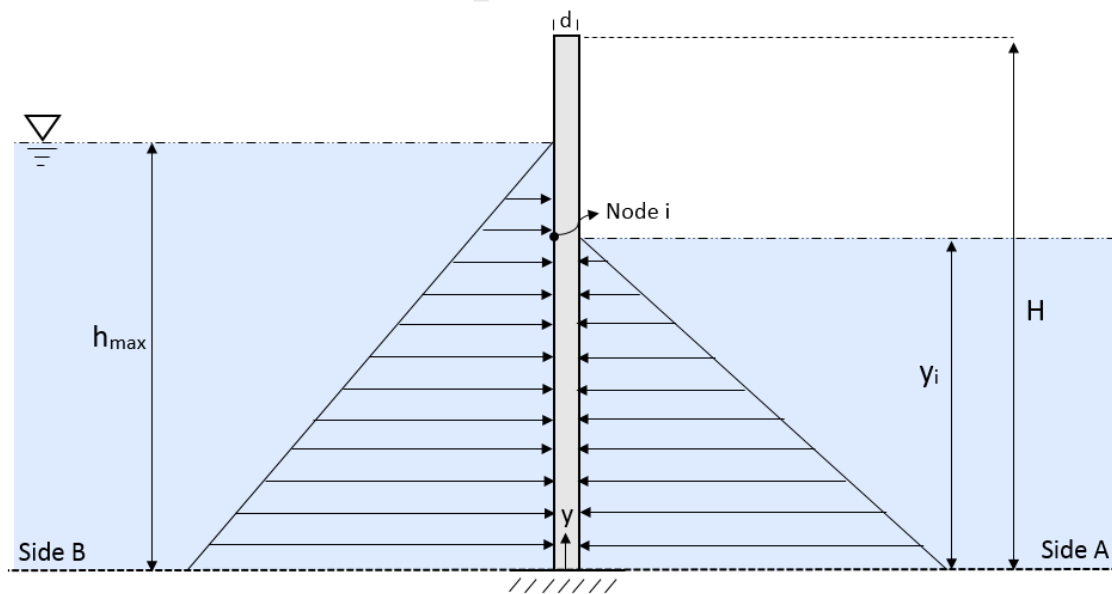


Figure 7- Cofferdam Sheet pile model for the TSFEM algorithm.

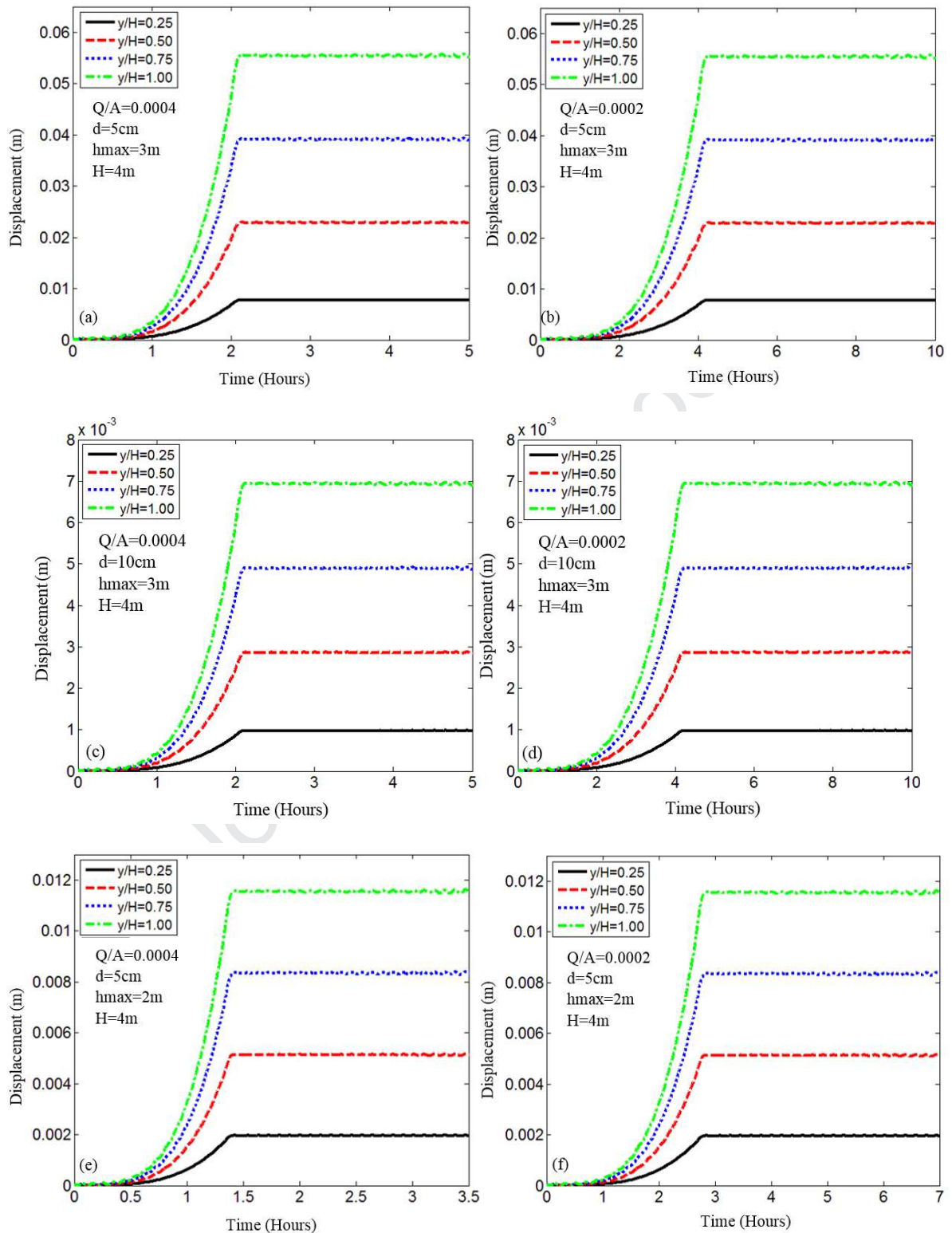


Figure 8- Horizontal Displacement of sheet pile wall with time due to flood pressure increment. Q is the volumetric flow rate, A is the reservoir area behind sheet pile, d is the wall thickness, h_{\max} is the maximum allowed water height and H is the wall height.

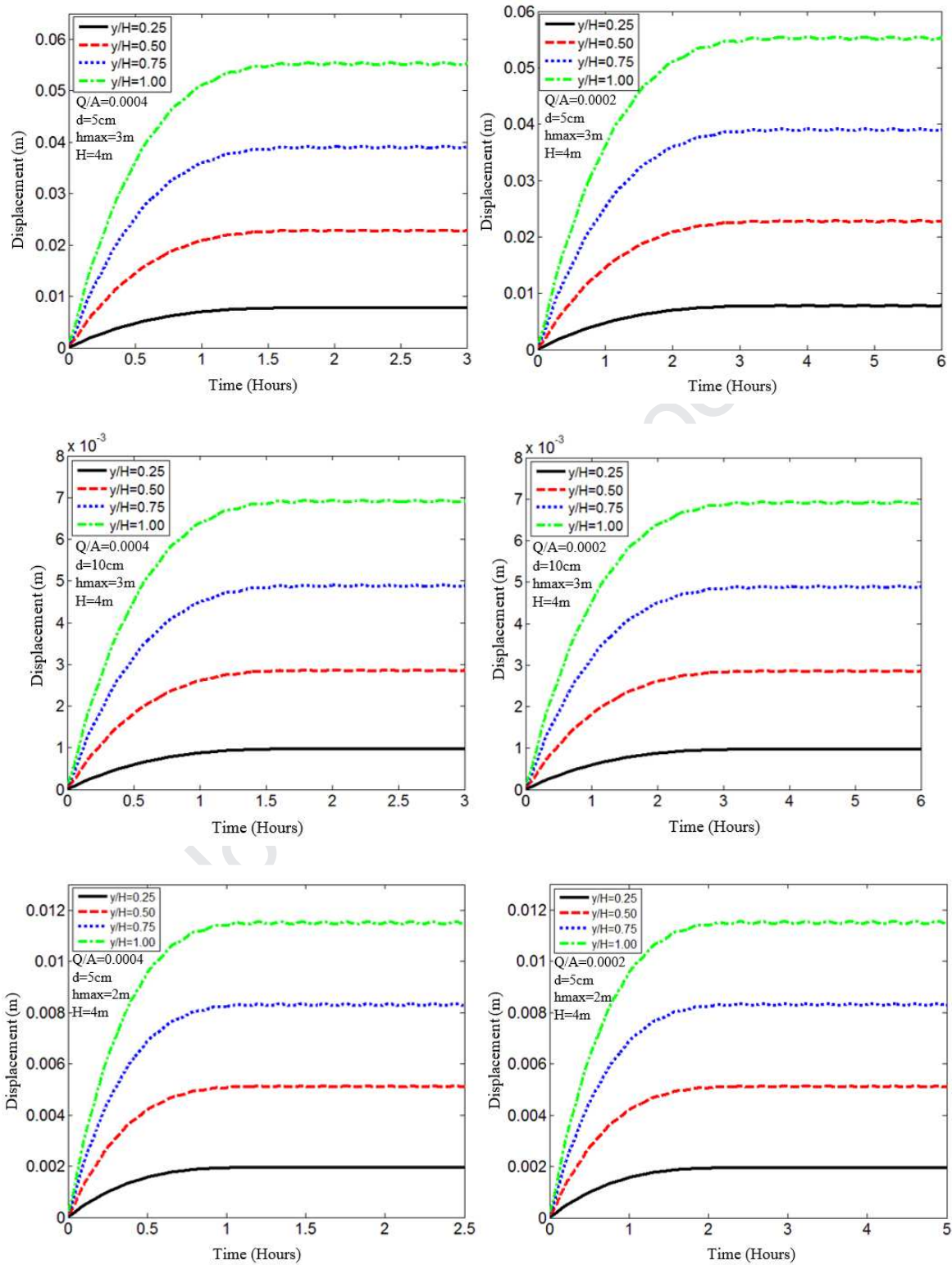


Figure 9- Horizontal Displacement of cofferdam sheet pile wall with time due to pumping out the water. Q is the volumetric flow rate, A is the inside area of the cofferdam, d is the wall thickness, h_{max} is the maximum water height and H is the wall height.

- Introducing the method of time series finite element analysis.
- Using Taylor and Fourier series for solving finite element boundary value problems.
- Using time series finite element method for solving wave propagation problem and obtaining natural frequencies.
- Using time series finite element method for solving geotechnical problems.



Journal Pre-proof

Manuscript title: ***A Time Domain Finite Element Approach Based on Time Series Estimation***

The authors whose names are listed immediately below certify that they have NO affiliations with or involvement in any organization or entity with any financial interest (such as honoraria; educational grants; participation in speakers' bureaus; membership, employment, consultancies, stock ownership, or other equity interest; and expert testimony or patent-licensing arrangements).

Author names: Alireza Firoozfar, Bahman Ansari

Conflicts of Interest Statement This statement is signed by all the authors to indicate agreement that the above information is true and correct (a photocopy of this form may be used if there are more than 10 authors):

Author's name	Author's signature	Date
Alireza Firoozfar		2019/11/01
Bahman Ansari		2019/11/01